16th IFAC Symposium on System Identification
The International Federation of Automatic Control
Brussels, Belgium. July 11-13, 2012

Control-Oriented Modeling of Motorcycle Dynamics ⋆

Matteo Corno, Pierpaolo De Filippi, Valerio Turri *
Giulio Panzani and Sergio M. Savaresi *

* *Dipartimento di Elettronica e Informazione, Politecnico di Milano, Piazza L. da Vinci 32, 20133 Milano, Italy. (email: {corno,defilippi, turri, panzani, savaresi}@elet.polimi.it).*

Abstract: Recent technology advances in the field of ride-by-wire technology for motorcycle (namely active braking and full electronic throttle) open the way to the design of innovative control strategies to improve two-wheeled vehicles stability. As such, it is of growing importance to devise control oriented models of the bike dynamics to be employed for control design purposes. This paper proposes an analytical model of a two-wheeled vehicle tuned to capture the coupling between longitudinal variables (i.e. traction and braking torque) and out-of-plane modes. The model is derived from first principles. The model parameters are identified from a complete multi-body simulator. The proposed model offers a good tradeoff between complexity and accuracy.

1. INTRODUCTION

Active chassis control systems (*i.e.*, traction and braking control systems, semi-active suspensions) are common in most commercial cars. In two-wheeled vehicles, instead, these control systems are being developed with a significant time delay. This is due to many factors: cultural, economical and technological. For example, motorcycle riders do not usually accept electronic control systems that may alter the natural riding feeling. Moreover, the market of two-wheeled vehicles is smaller than that of four-wheeled vehicles and thus motorcycle manufacturers have less resources to dedicate to research and development. Finally and most interesting from the technological point of view, motorcycle dynamics are more complex than four-wheeled vehicles one. In fact, in motorcycles in-plane and out-of-plane dynamics are coupled, Sharp [2001]. Therefore, the derivation of control-oriented models and to design model-based control systems is not trivial.

In the scientific literature several models of motorcycle dynamics have been derived, see Sharp [1971], Limebeer et al. [2001], Sharp et al. [2004, 2005], Cossalter and Lot [2002], Cossalter et al. [2004, 2010] and the reference therein. In these works, a multi-body approach has been adopted to derive models of the entire vehicle. For example, in Sharp et al. [2004] the vehicle has been considered composed of seven rigid bodies: front and rear wheel, front and rear unsprung mass, the chassis which includes the rider's lower body, the handlebar and the rider's upper body. The forces at the tire/road contact point are computed according to the Magic Formula (see Pacejka [2002]) and relaxation equations with a time-varying time constant. More recently, in Cossalter et al. [2010], several suspensions schemes, the flexibility of the sprocket absorber and a three degrees of freedom passive rider model have been considered. These models are suitable for simulation purposes and modal and sensitivity analysis, as they faithfully describe the dynamic behavior of the motorcycle. However, they are too complex to design model-based control systems.

The design of model-based control system requires models that are easily analyzed and can be synthetically described. For example in Tanelli et al. [2009], a 4th order model of the weave and wobble dynamics of the motorcycle has been derived. The model presented in that work was then used to design algorithms to control a semi-active steering damper (see De Filippi et al.).

Recently the concept of active stability control of two-wheeled vehicles has been introduced in De Filippi et al. [2010, 2011], where control strategies that increase the stability of the motorcycle by acting on the driving and braking torque have been presented. The controllers have been tuned on a black-box model identified from simulations performed in Bikesim^{TM}, an experimentally validated full-fledged commercial motorcycle simulation environment based on the AutoSim symbolic multi-body software Sharp et al. [2005], tuned to fit a high-performance motorcycle.

This work aims at providing a control-oriented model of the motorcycle dynamics that considers both longitudinal and lateral forces exerted by the tires and has as inputs the steering torque and the front and rear wheel torques. The proposed model is based on first principles and it is useful for control system design and for analyzing the interaction of the control system presented in De Filippi et al. [2010, 2011] with the vehicle parameters. To the best of authors' knowledge, the control-oriented models presented in the literature do not fit for this purpose, since they mainly focus on the design of steering controller and thus do not consider the wheel torques as input (see, for example Saccon et al. [2011], Getz [1995]). The model is validated against Bikesim^{TM}.

⋆ This work has been partially supported by MIUR project 'New methods for Identification and Adaptive Control for Industrial Systems'.

The rest of the paper is structured as follows: Section 2 is devoted to the derivation of the model, while Section 3 addresses parameters estimation and model validation on simulated data. Finally the paper is concluded with some remarks and an outlook to future work.

2. CONTROL-ORIENTED MODEL DERIVATION

In deriving the model, the vertical dynamics have been neglected, *i.e.*, the suspensions have been ignored and the longitudinal and lateral forces exerted by the tire at the contact point with the road have been linearized. Three different reference frames have been adopted to derive the model (see Figure 1):

- The inertial reference frame (XYZ): a right-handed time-unvarying reference frame fixed in the space;
- The body reference frame (xyz): a reference system fixed in the center of gravity of the main frame of the motorcycle with the z-axis parallel to the vehicle vertical axis and points upwards; the x-axis indicates the forward direction and the y-axis completes a right-handed frame.
- The intermediate reference frame ($X'Y'Z'$): a time-varying non-inertial reference system centered at the front wheel contact point. The Z'-axis is parallel to the Z-axis, the Y'-axis is perpendicular to both the Z- and x-axes, while the X'-axis completes a dextrose trio. This reference system can be obtained by rotating the inertial reference around the Z-axis by an angle equal to the yaw angle of the vehicle.

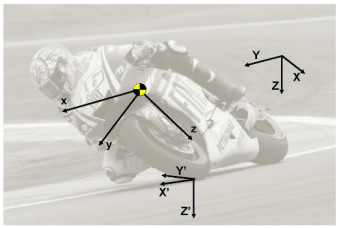

Fig. 1. Pictorial representation of the reference systems used to derive the model.

The model has 7 degrees of freedom (dof): the x position of the contact point between the rear tire and the road expressed in the inertial reference frame; the side-slip angle β of the vehicle calculated at the intersection of the vehicle vertical axis and the axis between the front and rear tire contact points; the yaw angle ψ of the vehicle expressed in the inertial reference frame; the roll angle φ of the vehicle expressed in the body reference frame; the steering angle δ; the front wheel angle ϑ_f and rear wheel angle ϑ_r. The input variables of the model are the rear wheel torque τ_{rw} (positive and negative); the front wheel torque τ_{fw} (negative) and the steering torque τ_s exerted by the rider. To derive the model, a force or torque balance has been written for each dof and two different equations have been added to evaluate the front and rear vertical loads that act on the wheels. In what follows, the symbols c_θ, s_θ and t_θ stand for $\cos(\theta)$, $\sin(\theta)$ and $\tan(\theta)$, respectively.

The torque balance (in the body reference frame) around the lateral axis of the front and rear wheel (see Figure 2) yields

$$J_{iwy}\ddot{\vartheta} = rF_{xi} + \tau_{iw},\ i = f, r \tag{1}$$

where J_{iwy} and r are the inertia and the radius of the wheel, respectively, and F_{xi} is the longitudinal force exerted by the tire defined as

$$F_{xi} = F_{zi}k_{\lambda i}\lambda_i,\ i = f, r, \tag{2}$$

and F_{zi} is the vertical load of the wheel, $k_{\lambda i}$ is the tire longitudinal stiffness and

$$\lambda = -\frac{\dot{x} + \vartheta_i r}{\dot{x}} \tag{3}$$

is the longitudinal slip. The chain pull effect is willingly neglected.

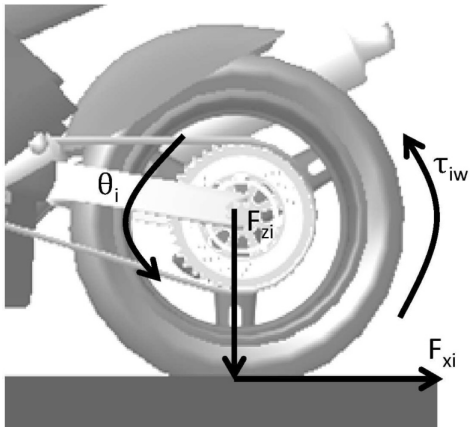

Fig. 2. Schematic view of the forces and torques acting at the wheel.

The torque balance computed around the steering axis in the body reference frame (see Figure 3) yields

$$\begin{aligned} J_s\ddot{\delta} =& s_\epsilon M_{xf} - J_{fwy}\dot{\vartheta}_f(c_\epsilon\dot{\varphi} + s_\epsilon c_\varphi\dot{\psi}) + \\ &+ c_\epsilon c_\varphi M_{zf} - (rs_\epsilon - d)c_\varphi F_{yr} + \\ &- (rs_\epsilon - d)s_\varphi F_{zf} - c_{steer}\dot{\delta} + \tau_s, \end{aligned} \tag{4}$$

where ϵ is the caster angle, c_{steer} is the damping coefficient of the steering damper and

$$M_{xf} = F_{zf}rt_{fw}t_{\varphi+s_\epsilon\delta} \tag{5}$$

is the moment around the longitudinal axis due to the lateral displacement rt_{fw} of the front tire/road contact point. Note that in Equation (5) the term $\varphi + s_\epsilon\delta$ is the camber angle of the front wheel (see Cossalter [2002]). Moreover, in Equation (4), the term

$$M_{zf} = F_{zf}(k_{mzfc}(\varphi + s_\epsilon\delta) + k_{mzf\alpha}\alpha_f) - F_{xf}rt_{fw}t_{\varphi+s_\epsilon\delta} \tag{6}$$

is the moment around the vertical axis. This term includes two contributions: the former depends on the front wheel camber angle and the front wheel side-slip angle $\alpha_f = \delta - t_{\beta+b_m\dot{\psi}+\dot{x}}$ and works against alignment, the latter is due to the lateral deformation of the front tire and tends to align the plane of the tire in the direction of the velocity. Note that, in Equation (4), the lateral force

$$F_{yf} = F_{zf}(k_{\alpha f}\alpha_f + k_{cf}(\varphi + s_\epsilon\delta)) \tag{7}$$

linearly depends on the front tire side-slip angle and camber angle. Finally, the term $J_{fwy}\dot{\vartheta}_f(c_\epsilon\dot{\varphi} + s_\epsilon c_\varphi\dot{\psi})$ in Equation (4) is a gyroscopic moment generated by the roll and yaw motion and it tends to reduce the steering angle.

The longitudinal force balance in the body reference frame (see Figure 4) is given by

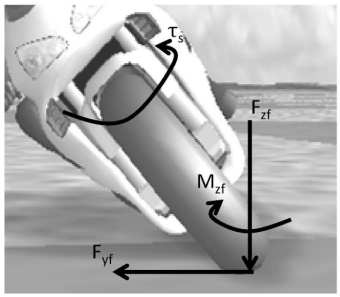

Fig. 3. Schematic view of the forces and torques acting at the steering assembly.

$$m_m \left[\ddot{x} - (\beta\dot{x} - h_m\dot{\phi}cos\phi)\dot{\psi}\right] = F_{xf} + F_{xr} + F_{drag}, \quad (8)$$

where m_m is the mass of the vehicle and rider, and $F_{drag} = -1/2\rho C_d A_{aero}\dot{x}^2$ is the drag force due to aerodynamic effects and it depends on the air density coefficient ρ, the drag coefficient C_d, the frontal cross section A_{aero} and the forward speed $\dot{x}$.

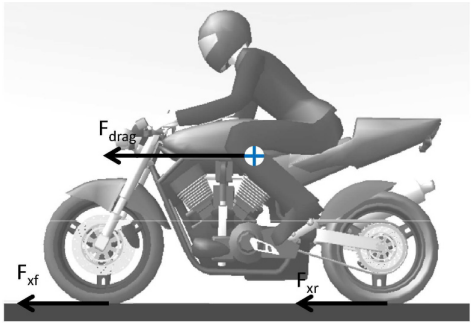

Fig. 4. Schematic view of the forces and torques acting at the chassis along the longitudinal direction.

The force balance along the lateral axis in the body reference frame (see Figure 5) yields

$$\begin{aligned} &m_m(\beta\ddot{x} + \dot{\beta}\dot{x}) + m_m(h_m c_\varphi\ddot{\varphi} - h_m s_\varphi\dot{\varphi}^2) = \\ &= -m_m\dot{x}\dot{\psi} + F_{yr} + F_{yf} - s_\varphi F_{lift}, \end{aligned} \quad (9)$$

where h_m is the height of the center of mass, $F_{lift} = -1/2\rho C_l A_{aero}\dot{x}^2$ is the lift force due to the aerodynamic (C_l is the lift coefficient) and

$$F_{yr} = F_{zr}(k_{\alpha r}\alpha_r + k_{cr}\varphi) \quad (10)$$

is the lateral force exerted by the rear tire at the contact point with the road. Note that, in this case, the camber angle of the rear tire is equal to the roll angle of the vehicle. Note that in equation (9), the term $\beta\ddot{x} + \dot{\beta}\dot{x}$ is the acceleration of the contact point between the vertical axis in the body reference frame and the axis between the front and rear tire contact points. The term $h_m c_\varphi\ddot{\varphi} - h_m s_\varphi\dot{\varphi}^2$, instead, is the acceleration of the center of gravity due to the roll motion of the vehicle, while $m_m\dot{x}\dot{\psi}$ is the centrifugal force acting at the center of gravity of the chassis.

Moreover, the torque balance computed around the longitudinal axis in the body reference frame (see Figure 6) is given by

$$\begin{aligned} &J_{mx}\ddot{\varphi} = M_{xr} + M_{xf} + J_{rwy}c_\varphi\dot{\psi}\dot{\vartheta}_r + \\ &+J_{fwy}(c_\varphi\dot{\psi} + c_\epsilon\dot{\delta})\dot{\vartheta}_f - h_m c_\varphi(F_{yr} + F_{yf}) + \\ &-h_m s_\varphi(F_{zr} + F_{zf}), \end{aligned} \quad (11)$$

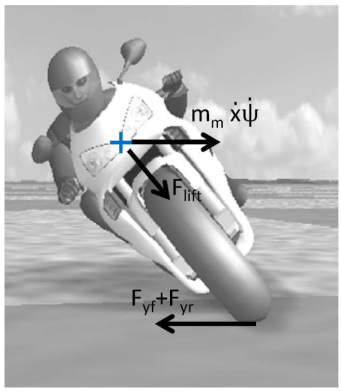

Fig. 5. Schematic view of the forces and torques acting at the chassis along the lateral direction.

where J_{mx} is the rotational inertia of the chassis around the longitudinal axis and

$$M_{zr} = F_{zr}(k_{mzrc}\varphi + k_{mzr\alpha}\alpha_r) - F_{xr}rt_{rw}t_\varphi \quad (12)$$

is the moment around the vertical axis due to the rear wheel force. This term, as the one due to the front wheel defined in Equation (5), includes two contributions: the former depends on the rear wheel camber angle and the rear wheel side-slip angle $\alpha_r = -\beta + t_{a_m\dot{\psi}/\dot{x}}^{-1}$ and works against alignment, the latter is due to the lateral deformation of the rear tire and it tends to align the plane of the tire in the direction of the velocity. Moreover, in Equation (11), the terms $J_{rwy}c_\varphi\dot{\psi}\dot{\vartheta}_r$ and $J_{fwy}(c_\varphi\dot{\psi} + c_\epsilon\dot{\delta})\dot{\vartheta}_f$ are gyroscopic moments due to the yaw motion that tend to stabilize the vehicle by decreasing the roll angle.

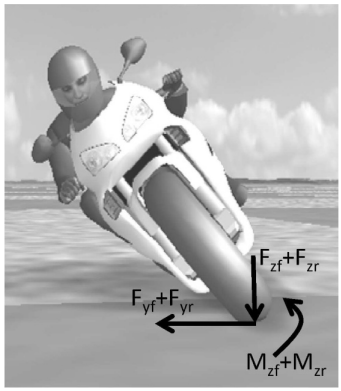

Fig. 6. Schematic view of the forces and torques acting at the chassis around the longitudinal axis.

Finally, the torque balance around the vertical axis of the intermediate reference frame (see Figure 7). With such reference frame, the vertical forces F_{zf} and F_{zr} do not generate a torque. Thus, the torque balance can be written as

$$\begin{aligned} &(J_{my}s_\varphi^2 + J_{mz}c_\varphi^2)\ddot{\psi} = M_{zr} + M_{zf} + \\ &-J_{fwy}\dot{\varphi}\dot{\vartheta}_f - J_{rwy}c_\varphi\dot{\varphi}\dot{\vartheta}_r + \\ &-a_m F_{yr} + h_m s_\varphi F_{xr} + b_m F_{yf} + h_m s_\varphi F_{xf} + s_\varphi M_{pitch}, \end{aligned} \quad (13)$$

where $M_{pitch} = 1/2\rho C_p A_{aero}L_w b\dot{x}^2$ is the pitching moment due to the aerodynamic forces, C_p is the pitch moment coefficient and $L_w b$ is the distance between the

center of pressure and the center of gravity. Note that this component is null if the motorcycle is ridden straight.

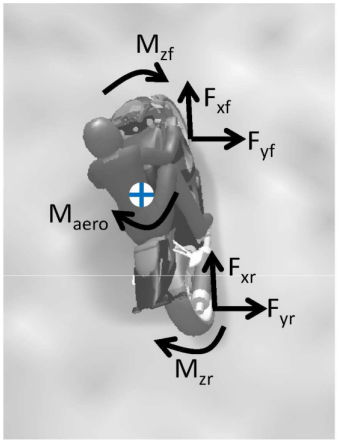

Fig. 7. Schematic view of the forces and torques acting at the chassis around the vertical axis.

To take into account the dynamic behavior of the tires, the tire relaxation length has been introduced in the computation of the side-slip angles, *i.e.*,

$$\dot{\alpha_i} = -\frac{\dot{x}}{L_{yi}}(\alpha_i - \alpha_{i0}),\ i = f, r \tag{14}$$

where L_{yi} is the tire relaxation length assumed to be constant and α_{i0} is the steady-state value of the side slip angle.

Equations (1)-(14) represent a 11th order nonlinear dynamical model, the state vector being

$$x = \left[\varphi\ \delta\ \dot{\varphi}\ \dot{\delta}\ \dot{x}\ \beta\ \dot{\psi}\ \dot{\vartheta}_r\ \dot{\vartheta}_f\ \alpha_r\ \alpha_f\right]'.$$

The nonlinear system depends on the front and rear vertical load. Thus, to solve the dynamical system, two additional equations are needed to evaluate the unknown vertical loads. To this end, the force balance along the vertical axis of the intermediate reference frame (see Figure 8)

$$m_m(h_m s_\varphi \ddot{\varphi} + h_m c_\varphi \dot{\varphi}^2) = m_m g + c_\varphi F_{lift} + F_{zr} + F_{zf} \tag{15}$$

has been considered, where $g = 9.81 m/s^2$ is the gravitational acceleration. Note that the term $h_m s_\varphi \ddot{\varphi} + h_m c_\varphi \dot{\varphi}^2$ is the lateral acceleration of the center of gravity.

The torque balance around the lateral axis of the intermediate reference frame yields

$$\begin{aligned} 0 = {} & a_m F_{zr} + h_m c_\varphi F_{xr} - b_m F_{zf} + h_m c_\varphi F_{xf} + \\ & + c_\varphi M_{aero} + J_{fwy} s_\varphi \dot{\varphi} \dot{\vartheta}_f + J_{rwy} s_\varphi \dot{\varphi} \dot{\vartheta}_r. \end{aligned} \tag{16}$$

By substituting in Equation (15) the expression of the roll angular acceleration given in Equation (11) and considering the linear dependency of the longitudinal and lateral forces on the vertical loads, starting from Equations (15)-(16) F_{zf} and F_{zr} can be expressed as a combination of the state variables.

By linearization the following linear model is obtained

$$\dot{x} = Ax + Bu, \tag{17}$$

where $u = [\tau_s\ \tau_{rw}\ \tau_{fw}]$ is the input vector.

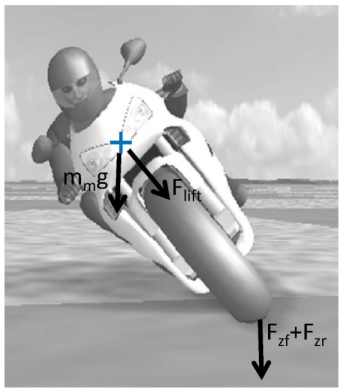

Fig. 8. Schematic view of the forces acting at the chassis along the vertical axis.

3. GRAY-BOX PARAMETERS IDENTIFICATION

Once the model has been derived, some parameters need to be estimated to evaluate the model effectiveness and suitability for control system design. The model analysis and a gray-box parameter identification have been performed using Bikesim as reference. Specifically, three different simulation experiments have been carried out, *i.e.*,

- sinusoidal sweep of the input steering torque;
- sinusoidal sweep of the front wheel torque;
- sinusoidal sweep of the rear wheel torque.

All the input signals range from 0.5 up to 20Hz and the simulations have been performed at a given constant forward speed $\dot{x} = 130 km/h$ with a roll angle $\varphi = 30°$. The roll angular rate time histories provided as outputs by the simulator and the model were considered for parameter identification purposes.

The employed parameter estimation procedure numerically minimizes the following cost function

$$J = \gamma_{\dot{\varphi}\tau_s} J_{\dot{\varphi}\tau_s} + \gamma_{\dot{\varphi}\tau_{rw}} J_{\dot{\varphi}\tau_{rw}} + \gamma_{\dot{\varphi}\tau_{fw}} J_{\dot{\varphi}\tau_{fw}} \tag{18}$$

where

$$J_{\dot{\varphi}u} = \sum_{k=1}^{N} (\dot{\varphi}_{sim}(k) - \dot{\varphi}_{mod}(k))^2,\ u = \tau_s,\ \tau_{rw},\ \tau_{fw}, \tag{19}$$

and the values of $\gamma_{\dot{\varphi}u}$ are selected to properly weight the cost functions. In Equation (19), N is the number of data, $\dot{\varphi}_{sim}$ and $\dot{\varphi}_{mod}$ are the simulator and model roll rate outputs, respectively.
Several parameters have been considered for optimization: in Appendix A the values of these parameters are collected in a table.

To validate the linear model (17), several simulations have been carried out. In Figure 9 the results obtained comparing the roll rate model output with the multi-body simulator one at $\dot{x} = 130 km/h$ in straight-running are depicted. The input of the system is an impulse-like steering torque performed by the rider. As can be seen, the agreement between the simulator and the model can be regarded as quite satisfactory.

As the cost function based on which the parameters were estimated considered explicitly the roll rate only, to further validate the model we compared the steer angle model output with the multi-body simulator one. The results

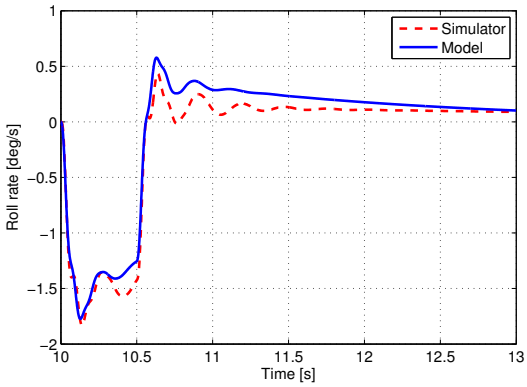

Fig. 9. Time history of the roll rate response to an impulse-like steering torque input: model (solid line) and simulator (dashed line).

are shown in Figure 10, where the model and simulated roll angle time responses are reported. As can be seen, also in a genuine validation test the agreement between the analytical model and the simulator can be regarded as very satisfactory.

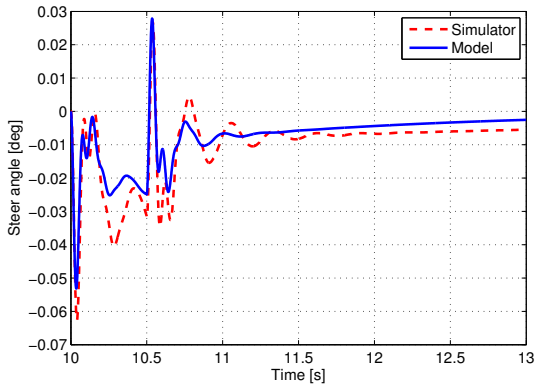

Fig. 10. Time history of the steering angle response to an impulse-like steering torque input: model (solid line) and simulator (dashed line).

Finally, in Figures 11 the time histories of the roll rate when the input is a step-like front wheel braking torque are depicted. This simulation has been carried out at a steady-state forward speed $\dot{x} = 130km/h$ with 30° of roll angle. As can be seen by inspecting the figures, the results are quite satisfactory also in this setting. Similar results have been obtained considering as input the rear wheel torque.

Since the A matrix in (17) strongly depends on the linearization point, wobble and weave strongly depends on the velocity and roll angle. Thus, to further validate the model, Figure 12 shows the map of the model eigenvalues as a function of the speed (the speed is increased from 50 to 170 km/h) and the roll angle (the roll angle is increased from 10 to 30 degrees). As can be seen, the weave and wobble modes characteristics are well captured by the model, and are in good agreement with what discussed in Sharp and Limebeer [2004], where a sport bike model was considered. Figure 12 shows that the weave mode moves, with the speed, within a frequency range of [1.4, 4.3]Hz,

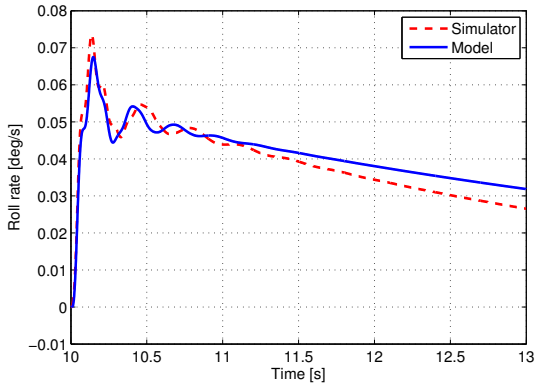

Fig. 11. Time history of the roll rate response to a step-like front wheel braking torque input: model (solid line) and simulator (dashed line).

whereas the wobble within approximately [7.8, 9.7]Hz. The damping of the weave mode consistently decreases as speed increases; this is true also for the wobble mode, even if the damping variation with speed is more limited. Moreover, the damping of these modes decreases as the roll angle increases: however, the damping is more sensitive to the forward speed than to the roll angle.

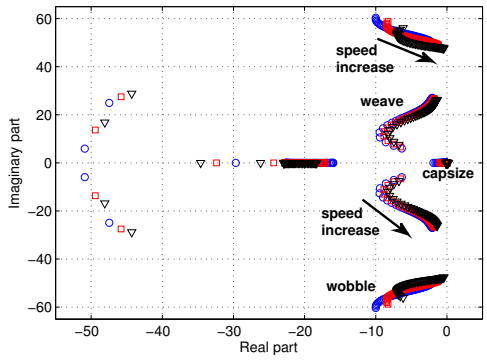

Fig. 12. Map of the model eigenvalues as a function of the speed and the roll angle: the speed is increased from 50km/h to 170km/h while the roll angle is 10° (circle), 20° (square), 30° (triangle).

Finally, Figure 13 depicts the map of the model eigenvalue as a function of the damping coefficient of the steering damper. The obtained results agree with the literature: higher the damping coefficient of the steering damper is, less damped the weave mode is and *vice versa*. The capsize mode is not influenced by the steering damper.

4. CONCLUDING REMARKS AND OUTLOOK

In the present paper a control oriented model of the motorcycle dynamics has been derived. The model has been derived with the specific goal of a model as simple as possible but able to capture all the dynamics relevant to active stability control of two-wheeled vehicles. For this reason tyre dynamics and tyre force have been explicitly considered. The resulting model is an 11^{th} order nonlinear system. Although seemingly high in order, the

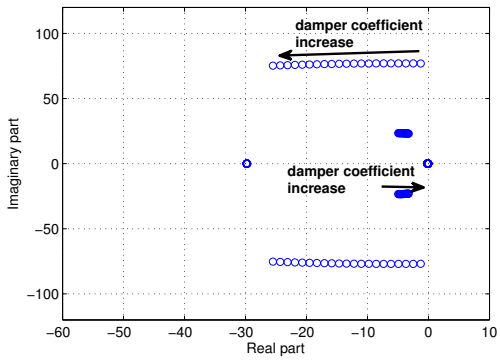

Fig. 13. Map of the model eigenvalues as a function of the damping coefficient of the steering damper obtained at high speed ($\dot{x} = 130$km/h) and 30° of roll angle.

Parameter	Initial value	Final value
m_m $[kg]$	274.8	274.8
a_m $[m]$	0.723	0.723
b_m $[m]$	0.647	0.647
h_m $[m]$	0.5	0.573 (+14%)
r $[m]$	0.278	0.278
ϵ $[deg]$	27.72	27.72
J_{mx} $[Nm^2]$	17	17
J_{mz} $[Nm^2]$	30	26.56 (-11%)
J_{my} $[Nm^2]$	40	52.97 (+32%)
J_s $[Nm^2]$	0.41	0.43 (+6%)
J_{rwy} $[Nm^2]$	0.64	0.64
J_{fwy} $[Nm^2]$	0.48	0.48
$k_{\lambda r}$ $[-]$	23	23
$k_{\alpha r}$ $[rad^-1]$	11	13 (+18%)
k_{cr} $[rad^-1]$	0.87	0.87
$k_{mzr\alpha}$ $[rad^-1]$	0.2565	0.2565
k_{mzrc} $[rad^-1]$	0.0247	0.0247
rt_{rw} $[-]$	0.0603	0.0603
$k_{\lambda f}$ $[-]$	26	26
$k_{\alpha f}$ $[rad^-1]$	12.36	16.13 (+30%)
k_{cf} $[rad^-1]$	1.11	1.11
$k_{mzf\alpha}$ $[rad^-1]$	0.2565	0.2565
k_{mzfc} $[rad^-1]$	0.0247	0.0247
rt_{fw} $[-]$	0.0388	0.0388

Table 1. Numerical values of the vehicle parameters

availability of the actual equations represents an advantage with respect to the classical Jacobian linearization approach commonly used in the literature. The model can be employed with advanced nonlinear model-based control system design and analysis tools.

5. VALUES OF THE MODEL PARAMETERS

See Table 1.

REFERENCES

V. Cossalter. *Motorcycle Dynamics*. Race Dynamics, Milwaukee, USA, 2002.

V. Cossalter and R. Lot. A motorcycle multi-body model for real time simulations based on the natural coordinates approach. *Vehicle System Dynamics: International Journal of Vehicle Mechanics and Mobility*, 37: 423–447, 2002.

V. Cossalter, R. Lot, and F. Maggio. The modal analysis of a motorcycle in straight running and on a curve. *Meccanica*, 39(1):1–16, 2004.

V. Cossalter, R. Lot, and M. Massaro. An advanced multibody code for handling and stability analysis of motorcycles. *Meccanica*, pages 223–233, 2010.

P. De Filippi, M. Tanelli, M. Corno, S.M. Savaresi, and L. Fabbri. Semi-active steering damper control in two-wheeled vehicles. *, IEEE Transactions on Control Systems Technology*, (99):1–18.

P. De Filippi, M. Tanelli, M. Corno, and S.M. Savaresi. Towards electronic stability control for two-wheeled vehicles: a preliminary study. In *Proceedings of the 10th ASME Dynamic Systems and Control Conference (DSCC)*, 2010.

P. De Filippi, M. Tanelli, M. Corno, and S.M. Savaresi. Enhancing active safety of two-wheeled vehicles via electronic stability control. In *Proceedings of the 18th IFAC world congress on automatic control*, pages 638–643, 2011.

N. Getz. *Dynamic inversion of nonlinear maps with applications to nonlinear control and robotics*. PhD thesis, Dept. Electr. Eng. and Comp. Sci., Univ. Calif., Berkeley, CA, 1995.

D.J.N. Limebeer, R.S. Sharp, and S. Evangelou. The stability of motorcycles under acceleration and braking. *Proc. I. Mech. E., Part C, Journal of Mechanical Engineering Science*, 215:1095–1109, 2001.

H.B. Pacejka. *Tyre and Vehicle Dynamics*. Buttherworth Heinemann, Oxford, 2002.

A. Saccon, J. Hauser, and A. Beghi. Trajectory exploration of a rigid motorcycle model. *IEEE Transactions on Control Systems Technology*, 2011. Available on line.

R. S. Sharp. Stability, control and steering responses of motorcycles. *Vehicle System Dynamics*, 35:291–318, 2001.

R. S. Sharp, S. Evangelou, and D.J.N. Limebeer. Multibody aspects of motorcycle modeling with special reference to Autosim. In *Advances in Computational Multibody Systems*, volume 2 of *Computational Methods in Applied Sciences*, pages 45–68. Springer Netherlands, 2005.

R.S. Sharp. The stability and control of motorcycles. *Journal of Mechanical Engineering Science*, 13:316–329, 1971.

R.S. Sharp and D.J.N. Limebeer. On steering wobble oscillations of motorcycles. *Proceedings of the Institution of Mechanical Engineers, Part C: Journal of Mechanical Engineering Science*, 218(12):1449–1456, 2004.

R.S. Sharp, S. Evangelou, and D.J.N. Limebeer. Advances in the modeling of motorcycle dynamics. *Multibody System Dynamics*, 12:251–283, 2004.

M. Tanelli, M. Corno, P. De Filippi, S. Rossi, S.M. Savaresi, and L. Fabbri. Control-oriented steering dynamics analysis in sport motorcycles: modeling, identification and experiments. In *Proceedings of the 15th IFAC Symposium on System Identification (SYSID), Saint Malo, France*, pages 468–473, 2009.